BUTTERWORTH HEINEMANN

Polymer Vol. 36 No. 9, pp. 1843–1848, 1995

0032-3861/95/$10.00+0.00

X-ray microscopy in polymer science: prospects of a 'new' imaging technique*

H. Ade† and A. P. Smith
Department of Physics, North Carolina State University, Raleigh, NC 27695-8202, USA

and S. Cameron
Exxon Research and Engineering, Annandale, NJ 08801, USA

and R. Cieslinski and G. Mitchell
ASL, Dow Chemical, Midland, MI 48667, USA

and B. Hsiao
Experimental Station, DuPont, Wilmington, DE 19880-0302, USA

and E. Rightor
Texas Polymer Center, B-1470, Dow Chemical, Freeport, TX 77541, USA

A relatively non-invasive imaging technique, which employs highly focused, tunable X-rays, is described. This technique—scanning transmission X-ray microscopy—can be used to investigate the bulk characteristics of polymeric materials with chemical sensitivity at a spatial resolution of about 50 nm. We present examples ranging from unoriented multiplase polymers to highly oriented Kevlar fibres. In the case of oriented samples, a dichroism technique is used to determine the orientation of specific chemical bonds. Extension of the technique to investigate surfaces of bulk samples is discussed.

(Keywords: X-ray microscopy; STXM; bulk characteristics)

INTRODUCTION

Although soft X-ray microscopy has been developed over many years, it is a relatively new imaging technique in the field of polymer science. Many of the X-ray microscopy developments since the late 1970s were driven primarily by the potential to image wet and unstained biological samples. (For a review of the established methods and developments over the last decade, see sources cited in ref. 1.) Recent developments of utilizing X-ray microscopy for polymeric systems are related to the realization that chemical sensitivity can be achieved in an X-ray microscope by operating the instrument at characteristic photon energies in the vicinity of an absorption edge. One is then able to differentiate spatially a variety of chemical compounds that have a very similar elemental make-up and density[2]. This is of interest, for example, for the characterization of multiphase polymers whose ultimate bulk and surface properties are strongly tied to their morphology. Light and electron microscopies are often successfully used to characterize such morphologies, but these techniques are inherently limited in their applicability and versatility, particularly in terms of chemical sensitivity (LM—resolution, contrast; EM—radiation damage, vacuum, contrast). In some circumstances not only is it necessary to visualize the morphology but detailed chemical (not just elemental) knowledge about the various domains is essential. For example, point spectra as acquired with the X-ray microscope can be used to provide chemical information about precipitates of unknown chemical composition. This is generally facilitated by comparing the spectra to those of model compounds.

As many readers are possibly unfamiliar with X-ray microscopy, we first describe some of the hardware and general performance of the X-ray microscope at the National Synchrotron Light Source (NSLS) at Brookhaven National Laboratory (BNL). We then illustrate the microscope's chemical sensitivity with a few examples. We furthermore discuss the polarization dependence of the near-absorption-edge cross-sections, and illustrate how this can be used to image the orientation of specific chemical bonds in a polymeric sample.

THE SCANNING TRANSMISSION X-RAY MICROSCOPE AT BROOKHAVEN NATIONAL LABORATORY

The Scanning Transmission X-ray Microscope at beamline X1A (X1-STXM) at Brookhaven National Laboratory has been conceived and developed over the last decade by the Stony Brook group led by J. Kirz[3]. It utilizes as its

* Presented at 'Aspects of Imaging in Polymer Science', 51st Annual Meeting of the Microscopy Society of America, 1–6 August 1993, Cincinnati, OH, USA

† To whom correspondence should be addressed

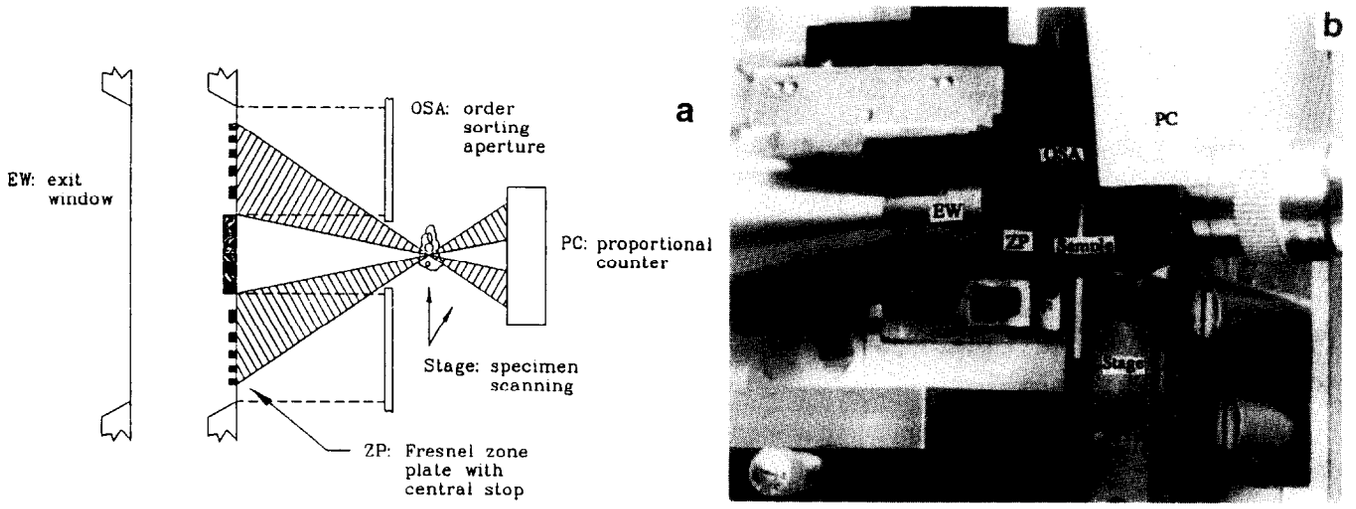

Figure 1 The X1 Scanning Transmission Microscope. (a) Schematic of its major components. (b) A photograph of the microscope in which the components indicated in (a) have been separated to distances much larger than during operations to facilitate identification of the various parts. The proportional counter has been raised above the optical axis, which is typically done to prealign the specimen with the visible light microscope at the right. (Figure courtesy of J. Kirz and C. Jacobsen, SUNY, Stony Brook)

source a high-brightness undulator installed in an electron storage ring at the National Synchrotron Light Source (NSLS). The X-ray beam is guided through a 24 m long evacuated beamline with the use of grazing incidence optics. Along its way, the beam is monochromatized by a spherical grating monochromator to an energy width of typically 0.5 eV at the carbon K edge. The energy width is adjustable within the 0.2 to 2 eV range, by controlling the size of two slits in the beamline[4]. The conceptual design of the microscope is depicted in *Figure 1*, and has not changed much in recent years. The X-ray beam exits the vacuum through a window consisting of a thin Si_3N_4 membrane into an atmospheric-pressure environment, and illuminates a zone plate—a diffraction optical element—to form a microprobe. The zone plates are produced in a collaboration between LBL and IBM. Its parameters, such as the outermost zone width and zone radii, are crucial for the performance of the X1-STXM, and are carefully controlled during production with electron beam lithography techniques[5]. The dimensions of the outermost zone width, for example, determine the size of the microprobe and therefore the highest spatial resolution obtainable, while the placement of the zones is important for aberration-free imaging. The zone thickness determines the efficiency with which the X-rays are diffracted into the positive first order, which is generally used as the microprobe. Jacobsen *et al.*[6] have measured the first-order efficiency to be above 10% between the oxygen and carbon K edges, and can be as high as 14%. This is in good agreement with theory for the given parameters and indicates the high quality of the zone plates utilized. The imaging characteristics of a zone-plate-based X-ray microscope and its future improvements depend entirely on the precision achievable with the microfabrication technology employed for the manufacturing of the zone plates.

In order to eliminate undesired diffraction orders at the sample location, the zone plate is fabricated with a beam stop in its centre, and an order selecting aperture (OSA; really just a slightly smaller pinhole) is strategically placed in the geometric shadow of the stop (see *Figure 1*). The sample is mechanically raster-scanned in the first-order focal plane with piezoelectric transducers under computer control. The range of the transducers is 75 μm, and a capacitance micrometer provides positioning with a minimum step size of 4.8 nm via closed-loop feedback. The transmitted flux is detected in a gas flow counter in pulse-counting mode and recorded digitally. To determine the imaging capabilities and resolution limit with the present zone plates, Jacobsen *et al.* imaged a star-like test pattern of gold-plated spokes. While the Rayleigh resolution of the X1-STXM is 55 nm, features smaller than 35 nm can be observed[6]. The modulation transfer function derived from data acquired from the test pattern shows that there is information in these images up to 20 μm^{-1} in spatial frequency. The measured modulation transfer function is in good agreement with theoretical predictions. More details about the performance of the imaging system can be found in articles by Zhang *et al.*[7] and by Jacobsen *et al.*[6].

CHEMICAL SENSITIVITY VIA N.E.X.A.F.S. MICROSCOPY

With the advent of tunable X-ray sources from synchrotron radiation facilities, X-ray absorption spectroscopy has developed into a powerful characterization technique during the last decade. In absorption spectroscopy one tunes the photon energy across an absorption edge and measures the cross-section of the excitation of core electrons into low-lying unoccupied electronic states and resonances or into the vacuum continuum. The spectral features observed close to the absorption edge are referred to as 'near-edge X-ray absorption fine structure' (n.e.x.a.f.s.). It is a sensitive probe of the local chemical and electronic structure of the atom whose core electron was excited. At energies further away from the absorption edge one calls the modulation in cross-section due to the backscattering of the photoelectrons by nearest-neighbour atoms 'extended X-ray absorption fine structure' (e.x.a.f.s). E.x.a.f.s is primarily a geometric structural tool, giving insight into bond lengths and coordination numbers.

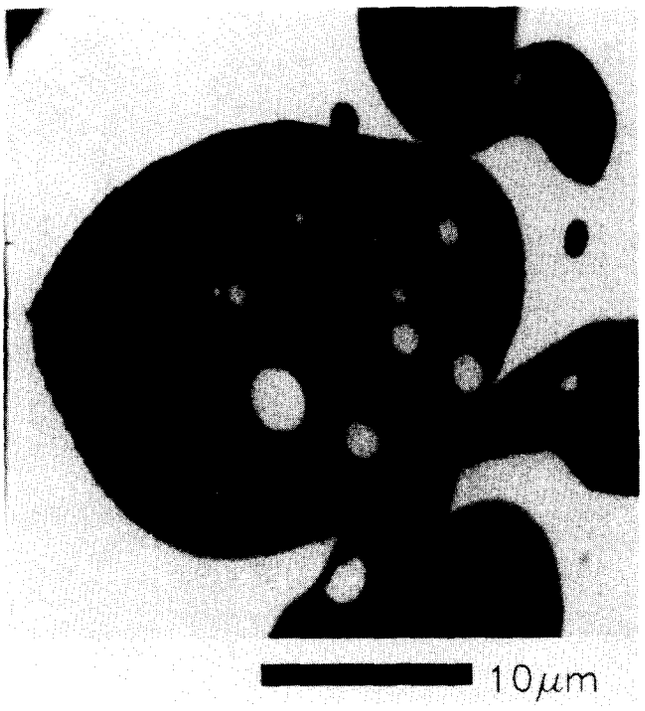

Figure 2 Micrograph of 0.5 μm thick section of poly(styrene-*r*-acrylonitrile)/polypropylene blend acquired at a photon energy of 285.5 eV. Styrene is strongly absorbing at this energy and the phase containing it appears dark, while polypropylene is virtually transparent. Black and white levels of the micrograph are from zero to incident intensity, i.e. contrast is not digitally or chemically enhanced. This micrograph was one of the very first to demonstrate the chemical capabilities of the X1-STXM

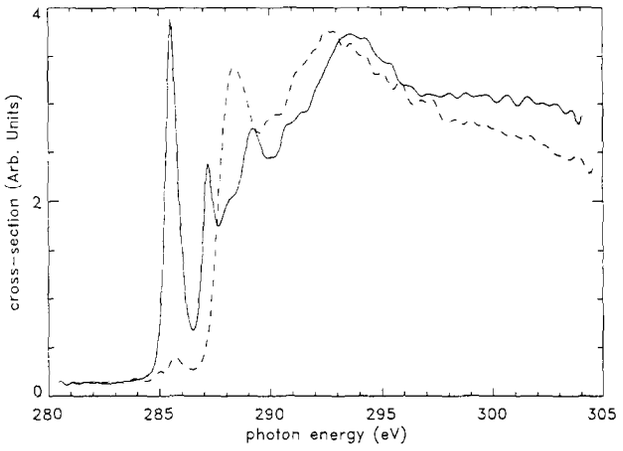

Figure 3 Carbon K-shell n.e.x.a.f.s. spectra of polypropylene (broken curve) and poly(styrene-*r*-acrylonitrile) (full curve) from small areas of the sample in *Figure 2*. The spectral feature at 285.5 eV is characteristic of an aromatic group, while the feature at 287.2 eV is due to nitrile. Acquisition time was 5 s, and the spectra were high-pass filtered in the Fourier domain[2]

Here, we are primarily interested in the n.e.x.a.f.s. of carbonaceous materials at the carbon K edge. Carbon n.e.x.a.f.s. has been successfully exploited to measure the unoccupied electronic structure of small organic molecules and polymers, as well as their bonding to and orientation on surfaces (see e.g. ref. 8). N.e.x.a.f.s. is particularly sensitive to distinguish saturated (sp^3 hybridization; σ bonds only) from unsaturated (sp^2, sp hybridization; σ and π bonds) bonding in these samples.

With judicious choice of photon energy, n.e.x.a.f.s. microscopy is capable of distinguishing among chemical functionalities such as C–C, C=C, C≡C, C=O, COOH and C≡N, as well as significantly more complex functionalities. To demonstrate this chemical sensitivity, we imaged several unstained multiphase polymers with very high contrast. In *Figure 2*, a poly(styrene-*r*-acrylonitrile)/polypropylene blend was imaged at a photon energy of 285.5 eV. At this energy styrene is highly absorbing, while the polypropylene matrix is practically transparent[2]. This micrograph has been among the very first to demonstrate the chemical imaging capabilities of the X1-STXM. Spectra of the two domains are shown in *Figure 3*, and one can readily see that at almost any photon energy there are some differences in the absorption cross-section with by far the largest difference at the so-called π^* resonance of styrene at 285.5 eV. Given the spectral difference and a sample thickness of about three absorption lengths, it is not surprising that the contrast $(I_{max}-I_{min})/(I_{max}+I_{min})$ in *Figure 2* is above 95%.

An even more dramatic example of chemical sensitivity with the X1-STXM was achieved with a polycarbonate/poly(ethylene terephthalate) (70/30 PC/PET) blend. Spectra of the domains as acquired with the X1-STXM are shown in *Figure 4*, exhibiting a variety of spectral features. The PET spectrum has a first π^* peak at 285.3 eV, with a pronounced shoulder at about 285.8 eV, and a strong second peak at 289.1 eV, followed by various other transitions at higher energies (for previous electron energy-loss spectroscopic (e.e.l.s) work on PET and molecular analogues, see ref. 9). PC has a sharp π^* peak at 285.75 eV, followed by broader transitions between 287 and 292 eV. The correlation of the spectra with the observed contrast and absorption in images is an additional benefit of the microscope and can be used to verify the relative energy between the two spectra. As predicted by the spectra, contrast reversal with high contrast is observed between images of the 70/30 PC/PET blend acquired at 285.36 and 285.69 eV (see *Figure 5*), a

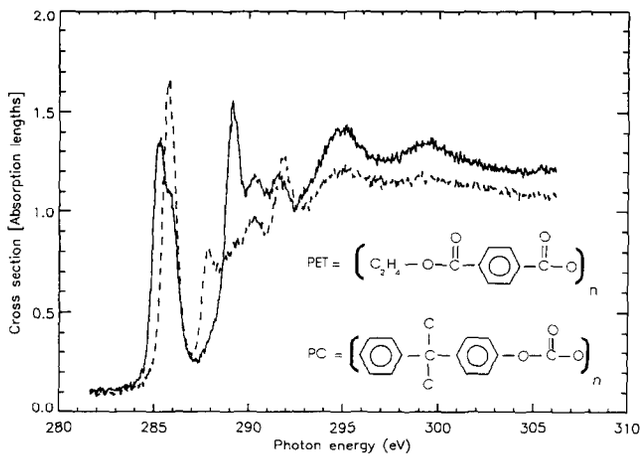

Figure 4 Spectra from 0.1 μm^2 area of a 70/30 PC/PET blend. A rich variation of spectral features between the two polymers is observed: PC, broken curve; PET, full curve[9]. In contrast to *Figure 3*, no filtering or smoothing of the data has been performed (see footnote on energy calibration)

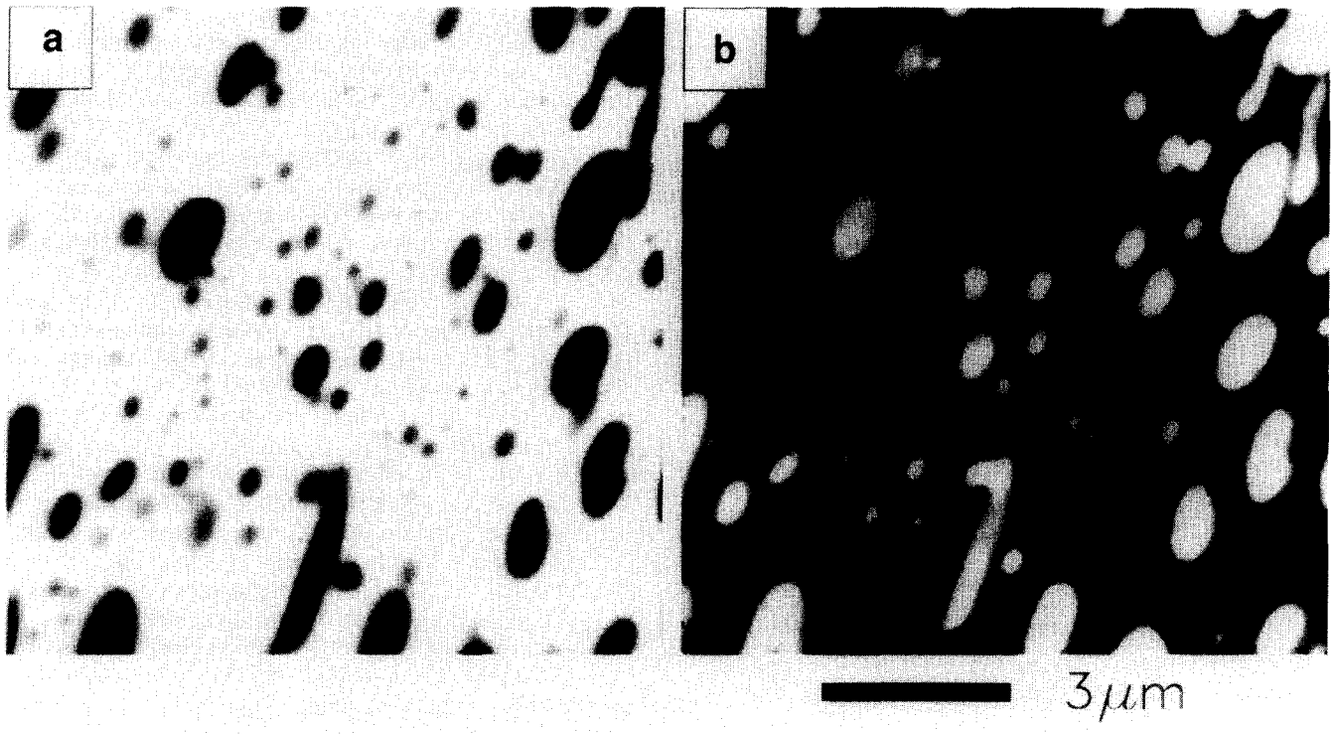

Figure 5 Micrographs of PC/PET blend acquired at a photon energy of 285.36 eV (a) and 285.69 eV (b) (see footnote on energy calibration). High contrast as well as contrast reversal with a photon energy change of less than 350 eV could be achieved

change in energy of less than 350 meV*. Unlike in *Figure 2*, contrast in this case is achieved by exploring subtle differences between resonances associated with the π bonds of the aromatic groups of each polymer. We note, however, that almost any photon energy would have resulted in some contrast between the two domains, with higher absorption for PC in three photon energy ranges, and higher absorption for PET in three complementary energy ranges. We have, for example, observed high contrast at 289.1 eV, which is particularly sensitive to the carbonyl groups of the PET.

SENSITIVITY TO BOND ORIENTATIONS

Besides the chemical sensitivity, n.e.x.a.f.s. is polarization-dependent[8]. The resulting X-ray linear dichroism can be used to image the orientation of specific bonds in (partially) ordered samples. We have explored this effect by investigating the radial structure of thin sections of poly(*p*-phenylene terephthalamide) (PPTA) fibres (Kevlar, DuPont registered trademark). A small-area spectrum of a Kevlar 49 thin film (0.1 μm thick) cut at 45° relative to the fibre axis as acquired with the X1-STXM is shown in *Figure 6*. The most prominent peaks are associated with aromatic (285.5, 286.3 eV) and carbonyl (288.3 eV)

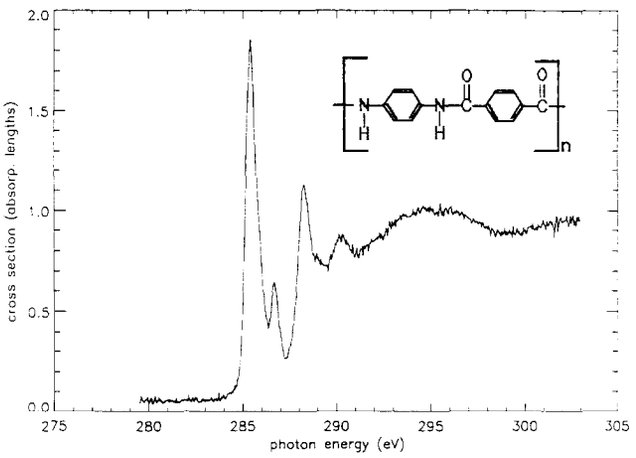

Figure 6 N.e.x.a.f.s. spectrum of 0.1 μm^2 area of 0.1 μm thick section of Kevlar 49 fibre cut at 45° as acquired with the X1-STXM. The prominent spectral features at 285.5, 286.7 and 288.3 eV are π^* resonances associated with unsaturated bonding in the aromatic and carbonyl groups, respectively. The energies are characteristic and provide for bond selective imaging, whereas the intensity depends on polarization and the geometrical orientation of the bonds. The broader feature at 295 eV is a σ^* resonance of the C–C bonds. Total acquisition time was 40 s

groups, and the photon energy can be selectively tuned to these characteristic energies to achieve chemical sensitivity during imaging. Owing to the polarization dependence of n.e.x.a.f.s., the strong peak at 285.5 eV, for example, would disappear if all the aromatic groups were to lie in a single plane and the electric field vector of a 100% polarized X-ray beam would also lie in the same plane (the aromatic π orbital is perpendicular to the

* The absolute energy calibration is not known to better than about 0.3 eV, and might vary slightly over some period of time. Energies quoted to a 'precision' better then 0.3 eV are therefore only relevant in the context of energy differences within the short time of the same experiment and sample. Since n.e.x.a.f.s. imaging and microspectroscopy are new operating modes of the X1-STXM, we are only now developing the necessary procedures to calibrate the monochromator easily with sufficient energy resolution. For the time being, we chose the π^* resonance of styrene to be at 285.5 eV, which is in reasonable agreement with the literature

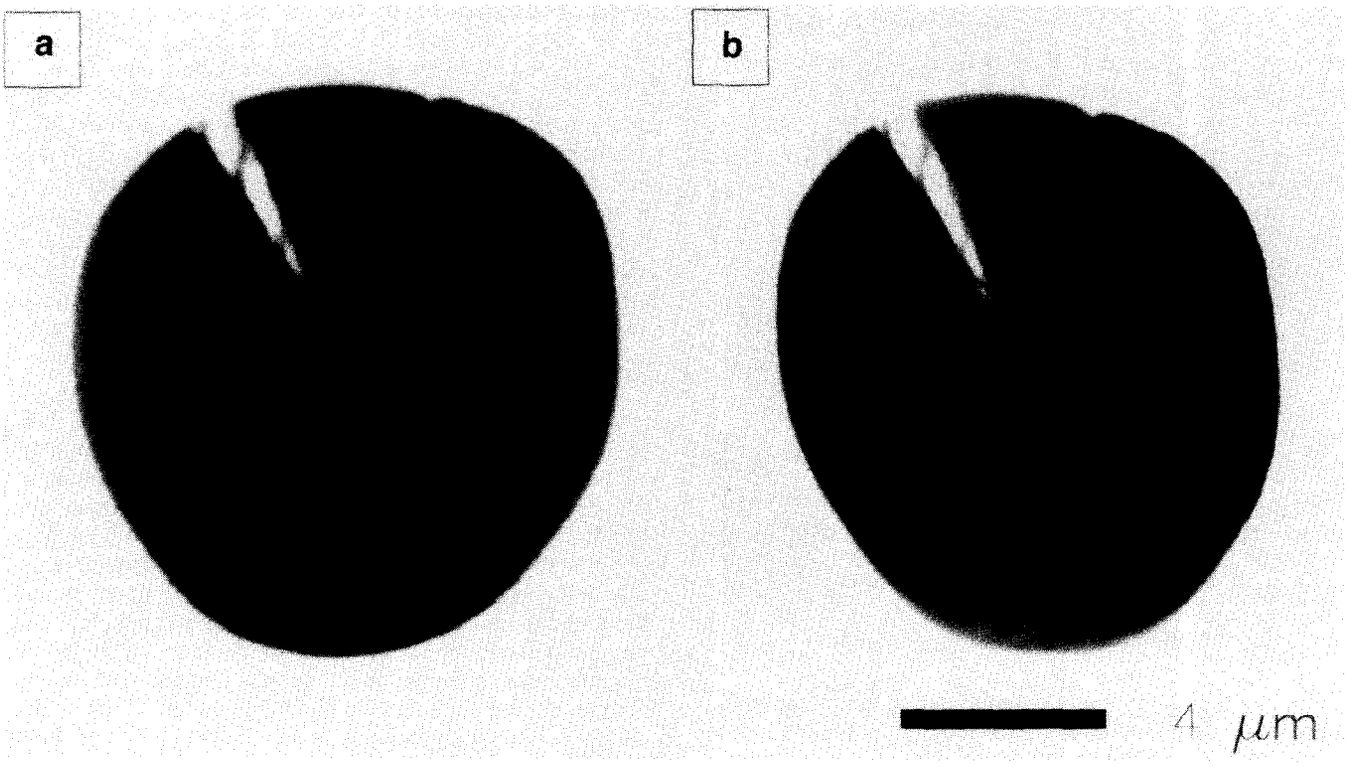

Figure 7 Micrographs of 200 nm thick Kevlar 149 fibre section (cut at 45° relative to fibre axis) imaged with electric field vector in left–right direction (a) and in up–down direction (b) at 285.5 eV photon energy. This energy selects the aromatic group of the fibre polymer and the butterfly patterns are due to the radial symmetry and orientational order of the fibre. The observed linear dichroism in these images is confirmed by the contrast changes between the two images

aromatic plane). The physics of this process in the case of π bonds is well understood. The intensity observed is proportional to $\cos^2\theta$, where θ is the angle between the electric field vector and the direction of the orbital excited during absorption[8]. *Figures 7a* and *7b* are micrographs of a 200 nm thick section of a Kevlar 149 fibre imaged with the electric field vector in the left–right direction (*7a*) and up–down direction (*7b*), respectively. A butterfly-like pattern with reversing contrast between the two images is readily discerned, as well as a crack in the fibre. Owing to the different orientation of the two aromatic groups within a repeat unit in this sample[10], the observable contrast is low[11]. The butterfly pattern is consistent with the structural model of Kevlar and the average aromatic ring plane pointing radially outwards. However, the degree of radial orientation varies for different Kevlar fibres. Future studies will be aimed at quantifying the radial order in various grades of Kevlar fibres. We will be able to study differences in orientation of carbonyl and aromatic groups using the ability to tune the photon energy to characteristic transitions.

POLYURETHANE FOAMS

For a number of years, phase segregation in flexible polyurethane foams has been a topic of considerable study by several techniques[12]. The chemistry of polyurethane foam formation is complex and depends on numerous variables. Segregated phases formed are typically small and not completely isolated from the surrounding matrix. This complexity makes chemical identification of morphological features of phase-segregated foams using microspectroscopic techniques such as STXM particularly challenging. We have begun studies of polyurethane foams based on methylene diphenyl diisocyanate (MDI), as precipitates are typically large and well segregated from the matrix. The phase morphology of a typical phase-segregated MDI-based foam is shown in *Figure 8*, which clearly shows the presence of a bimodal distribution of precipitate size. The larger precipitates are about 5 μm in size, while the smaller precipitates are less than 0.5 μm in this foam. As we have seen in STXM images of other aromatic polymers, a spectral feature at about 285 eV leads to a strong absorption of the X-ray beam. This is also true for the precipitates in the MDI foam, demonstrating that the precipitates are relatively rich in aromaticity, and that the matrix has a relatively high polyol functionality (aliphatic, R–O–R′). Previous studies on model MDI polyurethanes were carried out with electron energy-loss spectroscopy (e.e.l.s.) techniques with parallel detection[13], while e.e.l.s. applied in the gas phase is used to study molecular model compounds with structural units similar to those found in the respective polymers[9,14]. (This 'building-block' approach based on molecular analogues to interpret e.e.l.s. and n.e.x.a.f.s. spectra has been quite successful and is in most cases at least semiquantitative.) At high-spatial-resolution imaging, radiation damage becomes an important issue for radiation-sensitive materials such as polyurethanes. If valence-band transitions cause much of the damage, while core-level transitions provide the sought-after information, n.e.x.a.f.s. microscopy is estimated to have an advantage of about three orders of magnitude over e.e.l.s. imaging for polymeric samples[2].

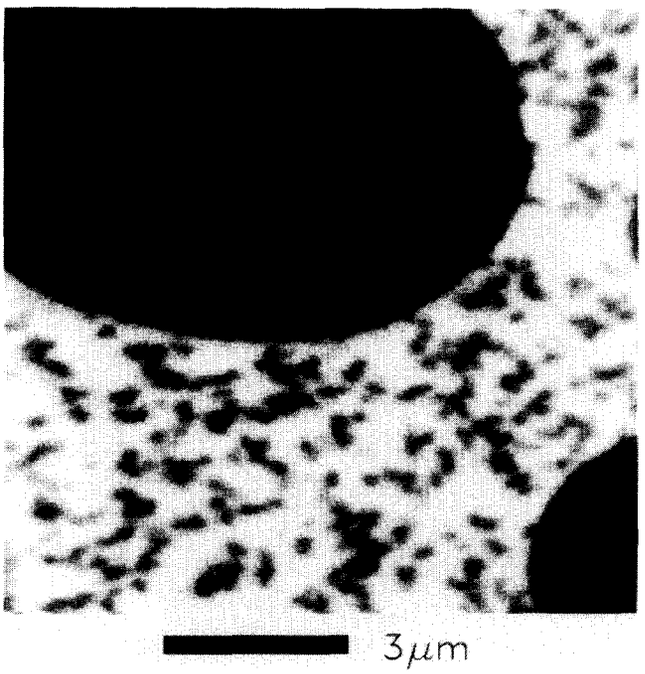

Figure 8 Micrograph of 200 nm thick section of a MDI-based polyurethane foam acquired at a photon energy of 285.5 eV where aromatic groups are highly absorbing. The dark precipitates, present in two different sizes, have thus a higher aromatic content than the matrix

SUMMARY AND PERSPECTIVE

We have shown how n.e.x.a.f.s. microscopy can be used to acquire high-spatial-resolution, high-contrast images for multiphase polymers. A variety of examples have been utilized to illustrate the uniqueness of the n.e.x.a.f.s. spectra for each polymer phase investigated, and how the spectroscopic differences in the near-edge region provide contrast. We have also shown how n.e.x.a.f.s. microscopy can be used to assess bond-orientational order by exploiting the linear polarization characteristics of synchrotron radiation and the polarization dependence of the near-edge spectral features. So far, we have predominantly employed the carbon K edge to acquire images and spectra, but the nitrogen, oxygen, chlorine and fluorine edges, as well as other core shells with energies in the 250–750 eV range, will eventually be exploited with the X1A microscope. The energy range from 250 to 390 eV is already easily accessible. Buckley *et al.*, for example, utilize the calcium L edge at about 350 eV in various bio-mineralization investigations[15], while Cody *et al.* observed chlorine in coal samples[16].

Utilizing detection techniques developed for n.e.x.a.f.s. spectroscopy without spatial resolution, it will be possible to make n.e.x.a.f.s. imaging surface-sensitive, probing selectively about 1 nm, 10 nm and 100 nm of the sample surface, by monitoring the near-edge cross-sections via the Auger, secondary electron and fluorescence yield, respectively. This would eliminate the need to prepare thin samples, necessary in many types of microscopes, and provide means to investigate the chemical and orientational characteristics of thick samples, such as fracture surfaces, directly. Surface-sensitive n.e.x.a.f.s. microscopy can furthermore be complemented with scanning photoemission microscopy[17], which is an inherently surface-sensitive technique.

We believe that the unique features presented and still to be explored, such as surface sensitivity, will make n.e.x.a.f.s. microscopy a valuable characterization tool in polymer science. N.e.x.a.f.s. microscopy with fluorescence detection should even be able, for example, to investigate a surface covered with a thin liquid overlayer. Additional microscopes soon to be completed at the Advanced Light Source in Berkeley will provide even higher energy resolution and increased intensity. The spatial resolution of X-ray microscopes will also improve as zone plate fabrication technology advances.

ACKNOWLEDGEMENTS

Part of this work was performed while HA was at SUNY, Stony Brook, and was supported by NSF Grant DIR 9005893. We thank J. Kirz, C. Jacobsen, S. Williams, X. Zhang, S. Wirick, H. Rarback, C. Buckley, E. Anderson, D. Attwood, D. Kern and M. Rivers for the development and maintenance of the X1-STXM. Furthermore, J. Kirz, C. Jacobsen, S. Williams, X. Zhang and M. Rivers have significantly participated in implementing the n.e.x.a.f.s. imaging mode. We would further like to thank S. Subramoney from DuPont, M. Dineen from Dow Chemical, and C. Costellp, E. Berluche, J. Chudzinsky and S. Behal from Exxon Research for providing samples and assisting in numerous ways. We thank B. Young for sectioning the polyurethane samples and R. Priester for thoughtful discussions on polyurethane chemistry. This work was performed at the NSLS, which is supported by the Department of Energy, Office of Basic Energy Sciences.

REFERENCES

1 'X-Ray Microscopy' (Eds G. Schmahl and D. Rudolf), Springer, Berlin, 1984; 'X-Ray Microscopy II' (Eds D. Sayre, M. Howells, J. Kirz and H. Rarback), Springer, Berlin, 1988; 'X-Ray Microscopy III' (Eds A. Michette, G. Morrison and C. Buckley), Springer, Berlin, 1992
2 Ade, H. *et al. Science* 1992, **258**, 972
3 Kirz, J., Burge, R. and Rarback, H. *Ann. N.Y. Acad. Sci.* 1980, **342**, 135; Kirz, J. *et al. Rev. Sci. Instrum.* 1992, **63**, 557
4 Rarback, H. *et al. J. X-Ray Sci. Technol.* 1992, **2**, 274
5 Anderson, E. and Kern, D. 'X-Ray Microscopy III' (Eds A. Michette, G. Morrison and C. Buckley), Springer, Berlin, 1992
6 Jacobsen, C. *et al. Opt. Commun.* 1991, **86**, 351
7 Zhang, X., Jacobsen, C. J. and Williams, S. P. 'Soft X-Ray Microscopy' (Eds C. Jacobsen and J. Trebes), *SPIE Proc.* 1992, **1741**, 251
8 Stohr, J. 'NEXAFS Spectroscopy', Springer, Berlin, 1992, and references therein; Sette, F., Stohr, J. and Hitchcock, A. P. *J. Chem. Phys.* 1984, **81**, 4906; Outka, D. A. *et al. Phys. Rev. Lett.* 1987, **59**, 1321; Tourillon, C. *et al. Surf. Sci.* 1988, **201**, 171
9 Hitchcock, A. P., Urquhart, S. G. and Rightor, E. G. *J. Phys. Chem.* 1992, **96**, 8736; Rightor, E. *et al. Microbeam Anal.* 1993, **2**, S264
10 Yang, H. H. 'Aromatic High Strength Fibers', Wiley-Interscience, New York, 1989; Dobb, M. D., Johnson, D. J. and Saville, B. P. *J. Polym. Sci., Polym. Phys. Edn* 1977, **15**, 2201
11 Ade, H. and Hsiao, B. *Science* 1993, **262**, 1427
12 Armisted, J., Wilkes, G. and Turner, R. *J. Appl. Polym. Sci.* 1988, **35**, 601; Okamoto, D., O'Connelki, E., Cooper, S. and Root, T. *J. Polym. Sci.* 1993, **31**, 1163
13 Urquhart, S. G., Hitchcock, A. P., Leapman, R. D., Priester, R. D. and Rightor, E. G. *J. Polym. Sci. B: Polym. Phys.* submitted
14 Urquhart, S. G., Hitchcock, A. P., Priester, R. D. and Rightor, E. G. *J. Polym. Sci. B: Polym. Phys.* submitted
15 Buckley, C. *et al. Rev. Sci. Instrum.* 1992, **63**, 588
16 Cody, G. personal communication
17 Ade, H. *et al. Appl. Phys. Lett.* 1990, **56**, 1841